03,11

Electronic band structure, charge density distribution and chemical bonding in molecular crystals of chalcogens

© V.G. Orlov[1,2], G.S. Sergeev[1]

[1] National Research Center „Kurchatov Institute“,
Moscow, Russia
[2] Moscow Institute of Physics and Technology (State University),
Dolgoprudnyi, Moscow Region, Russia

E-mail: valeryorlov3@gmail.com

Received June 27, 2022
Revised July 4, 2022
Accepted July 4, 2022

The electronic band structure and the charge density distribution are theoretically studied in rhombohedral and monoclinic selenium, rhombohedral and orthorhombic sulphur with the aim to classify types of chemical bonding in molecular crystals of chalcogens. It is found that valence *s*- and lower in energy *p*-electrons contribute mainly in covalent bonds between nearest neighboring atoms in ring-shaped molecules, while all types of valence *p*-electrons provide bonding between rings of atoms in crystals. Parameters of critical points and the character of the charge density distribution in their vicinity point to coexistence of a number of types of chemical bonding in molecular crystals of Se and S: covalent, semimetallic and one more type, characterizing by the charge density fluctuations. Van der Waals forces, being important for finding equilibrium lattice parameters, have little impact on the charge density distribution and on the chemical bonding in crystals of chalcogens.

Keywords: chalcogens, molecular crystals, electronic band structure, types of chemical bonding.

DOI: 10.21883/PSS.2022.12.54378.417

1. Introduction

Chalcogenes (S, Se, Te) and their compounds — semiconductor chalcogenides — are used in electronics, optics, radiation detection devices, in various types of computer memory, in power engineering, as well as in medicine, biology and many other areas of practical applications [1].

In recent years, much attention has been attracted by the unusual properties of the electronic band structure of trigonal Se and Te [2–7], due to the chiral symmetry (absence of spatial inversion and mirror-rotating axes) of their crystal lattice (spatial groups $P3_121$ or $P3_221$ [8]), the atoms in which are arranged in parallel screw chains forming a hexagonal structure [9,10]. The electronic structure of Te and Se is of significant interest for explaining the transport properties of efficient thermoelectrics [11]. The need to improve the parameters of Li-S, Na-S and K-S batteries aroused interest in the electronic properties of orthorhombic modification of sulfur α-S [12].

Trigonal Se and Te are not molecular crystals in the generally accepted understanding of this term, since there are no ring-shaped or any other closed molecular structures in their crystal lattice. But their electronic structure and features in the charge density distribution are important for understanding the properties of Se and S molecular crystals.

There is a wide range of opinions on the nature of the chemical bond in chalcogen crystals, as well as on the participation of valence *s*- and *p*-electrons in the formation of the bond between the elements of the crystal structure. In early studies [13–15], which used Pauling's ideas [16] about valence bonds, resonant bonding and about lone-pair electrons, a number of statements were made: 1) valence *s*-electrons can be ignored when considering the nature of the chemical bond in trigonal Se and Te, since their energies are significantly deeper compared to the energies of valence *p*-electrons (in contrast to sp^3 hybridization of *s*- and *p*-electrons in Ge and Si), 2) the states of valence *p*-electrons can be divided into two groups — the low-lying *p*-electrons that provide a covalent bond between the nearest neighboring atoms in the screw chains, and the overlying *p*-electrons of the lone pair that do not participate in the formation of bonds between atoms, 3) each atom in the chain is covalently bound to the two atoms closest to it of the same chains, while the bond with four atoms in neighboring chains of trigonal Se and Te has a resonant and Van der Waals character. But the latter statement was not accompanied by any estimates of the Van der Waals forces in Se and Te.

The empirical pseudopotential method and tight-binding models were used to calculate the electronic band structure and charge density distribution in trigonal Se and Te [17]. Based on the analysis of the charge density distribution in [17], a number of conclusions were made: 1) the covalent bond between neighboring atoms of spiral chains is due to the contribution of low-energy valence *s*- and *p*-electrons, 2) valence *p*-electrons with energies in the range from -3.5 to -2.2 eV are responsible for the connection between the spiral chains. The type of this bond was named as covalently similar (covalentlike), but significantly weaker compared to

the covalent bond between atoms in chains. The charge density distribution of the *p*-electrons of an unshared pair in [17] was not considered. The electronic band structure of trigonal Se and Te in [17] was calculated in a non-relativistic approximation, and the Van der Waals forces were not taken into account.

In the study [18], the essential role of valence *s*-electrons in the formation of bonds between neighboring atoms in the helical chains of the trigonal crystal structure Te was revealed. In agreement with the results of the article [17], in the study [18] it was shown that valence *p*-electrons are responsible for the bond between atoms, both in chains and between neighboring chains. But in [18] it was noted that due to the overlap of the zones of valence *p*-electrons in the trigonal Te, splitting them into two parts — binding and electrons of an lone pair — is possible only with a big error. In the article by the authors of [19] it was shown that, unlike trigonal Te, trigonal Se has underlying zones of valence p_l-electrons located in the energy range from -6 eV to -3 eV, practically do not overlap with the overlying zones of *p*-electrons (from -3 to 0 eV). This made it possible to determine the partial contributions of valence *s*-, p_l- and p_u-electrons to the charge density of ρ_b saddle critical points of the bond type (bond critical points, BCPs) in the charge density distribution in trigonal Se. It turned out that valence *s*- and p_l-electrons make the main contribution to ρ_bBCPs of the first type covalently binding the nearest neighboring atoms of helical chains, while valence p_l- and p_u-electrons define ρ_bBCPs of the second type, connecting the atoms of the helical chain with the atoms of the four neighboring helical chains closest to it. The similarity of the parameters of BCPs of the second type in trigonal Se and Te with the parameters of similar BCPs in the semimetallic Sb, as well as the similarity of the nature of the charge density distribution in the vicinity of these BCPs allowed us to conclude that two types of chemical bonds in trigonal Se and Te — covalent and semimetallic [18,19] coexist. It was also shown in [19] that Van der Waals forces in trigonal Se and Te have little effect on the BCPs' parameters that determine the nature of the chemical bond in these crystals.

The electronic band structure of trigonal Se and Te was calculated in [19] using the WIEN2k [20,21] computer software package. As an exchange potential, the modified by Tran and Blaha [22] exchange potential of Becke and Johnson (mBJ) was used. Short-range correlations were taken into account in the local density approximation (LDA). In [19], theoretical values of the energy gaps for trigonal Se and Te were obtained, close to experimental ones, and the structure of the upper valence bands and lower bands of conduction electrons, essential for explaining the topological properties of the electronic structure of trigonal Se and Te [2–7], was correctly reproduced.

Given the great attention to the properties of two-dimensional [23] and layered [24] inorganic molecular crystals in connection with the potential possibilities of their practical use, it was of interest to carry out calculations and analysis of the electronic band structure of molecular chalcogen crystals, also having a layered character of the crystal structure. From the known allotropic modifications of molecular chalcogen crystals, the most stable at normal pressure rhombohedral modifications Se_6 [25] and S_6 [26], monoclinic α-Se_8 [27] and orthorhombic α-S_8 [28], were selected for calculations, the structural units of which are, respectively, six-branched and eight-branched molecules from Se and S atoms. Under normal conditions, Te has only one known type of equilibrium crystal structure — trigonal [10], which, as noted above, does not apply to molecular crystals. In this paper, both similarities and differences in the electronic structure and types of chemical bonds realized in molecular crystals Se and S and in trigonal Se and Te are noted.

2. Calculation methods

The results described in this article were obtained using a complex of computer programs WIEN2k [20,21] used to calculate the electronic band structure of rhombohedral Se and S, monoclinic α-Se, orthorhombic α-S, as well as to find the charge density distribution $\rho(\mathbf{r})$ in the crystal lattices of the chalcogens mentioned above. One of the most difficult problems of applying the density functional theory (DFT) to study physical properties is the proper choice of the exchange-correlation functional. The main results of this paper are obtained using the modified by Tran and Blaha [22] Becke and Johnson exchange potential (mBJ), which gives the values of energy gaps in semiconductors and oxides close to the experimental [29]. Short-range correlations were taken into account in the local density approximation (LDA). Calculations of the electronic band structure were carried out both with experimental values of crystal lattice parameters and with optimized lattice parameters. The exchange-correlation PBE functional (Perdew–Burke–Ernzerhof [30]) was used to optimize the crystal structure. The PBE functional is based on the Generalized Gradient Approximation (GGA) and is the second most complex functional out of a number of exchange-correlation functionals [31,32] used in DFT.

To identify the contribution of Van der Waals forces to the formation of chemical bonds in molecular chalcogen crystals, the nonlocal exchange-correlation functional rev-vdW-DF2 proposed by Hamada [33] was used. This functional has been tested on a large number of substances and has been recommended for use by [34], as giving the smallest error when calculating binding energies and optimizing the parameters of crystal structures.

For valence states, relativistic effects were taken into account by means of the variational method using spin-orbit interaction. The states of the core electrons were calculated by complete relativistic method [20]. To achieve the required accuracy, the following parameters were used: expansion in l-orbital momentum inside atomic spheres was carried out to the values of $l_{\max} = 10$, the largest values of the wave

vector k_{max} used for expansion by plane waves were found using the product $R_{mt}k_{max}$, equal to 6.5 and 8.5 for S and Se, respectively, where R_{mt} represents the radius of the atomic sphere. The total number of points in the Brillouin zone was taken to be 5000. The convergence criterion of the iterative calculation procedure for the total energy was 10^{-5} Ry.

To find critical points in the charge density distribution $\rho(\mathbf{r})$, the program CRITIC2 [35] was used, developed for topological analysis of scalar fields in periodic lattices based on the method „Quantum Theory of atoms in molecules" (QTAIM) [36–38]. The classification of critical points in the charge density distribution and their use for analyzing the nature of the chemical bond in crystals were described in detail in our papers [18,19]. As a result, we only briefly note that in the following presentation, the following BCPs [39] parameters will be used to classify the types of chemical bonds in chalcogen crystals: the eigenvalues λ_i Hesse matrix (matrix of the second derivatives of the charge density in coordinates), i.e. the main values of the curvature of Hesse matrix, the Laplacian of the charge density $\nabla^2\rho_b$, the value of the charge density ρ_b, as well as two dimensionless parameters — flatness f (flatness, the ratio of the minimum charge density in the critical a point of type cage ρ_c^{min} to the maximum charge density in BCPs ρ_b^{max}, which characterizes the uniformity of the charge density distribution in the crystal) and the molecularity

$$\mu = (\rho_b^{max} - \rho_b^{min})/\rho_b^{max}, \quad \nabla^2\rho_b^{max} \cdot \nabla^2\rho_b^{min} < 0.$$

3. Results

3.1. Density of energy states (DOS) and energy gap in chalcogen crystals at normal pressure

All chalcogen atoms have the same type of valence electron s^2p^4 configuration. Partial densities of energy states (DOS) for valence s- and p-electrons in rhombohedral and monoclinic Se, as well as in rhombohedral and orthorhombic S, calculated with experimental values of crystal lattice parameters, are shown in Fig. 1. For comparison, Fig. 1 also shows the previously found [18,19] DOS for trigonal Te and Se.

We note the most significant features of DOS in Fig. 1. The zones of s-electrons in rhombohedral Se and S, monoclinic α-Se and orthorhombic α-S are divided into several narrow subzones. Their number for these molecular crystals is exactly equal to the number of eigenvalues for the states of s-electrons in six- and eight-atom molecules Se and S (respectively, four and five) calculated in the articles [40–42] using the method of quantum chemistry CNDO/S (the method of Complete Neglect of Differential Overlap for Spectroscopy). In all allotropic modifications of Se, the upper zones of valence p_u-electrons, which in early works [14,17] were called p-electrons of the lone pair, are separated from the low-lying zones of p_l-electrons,

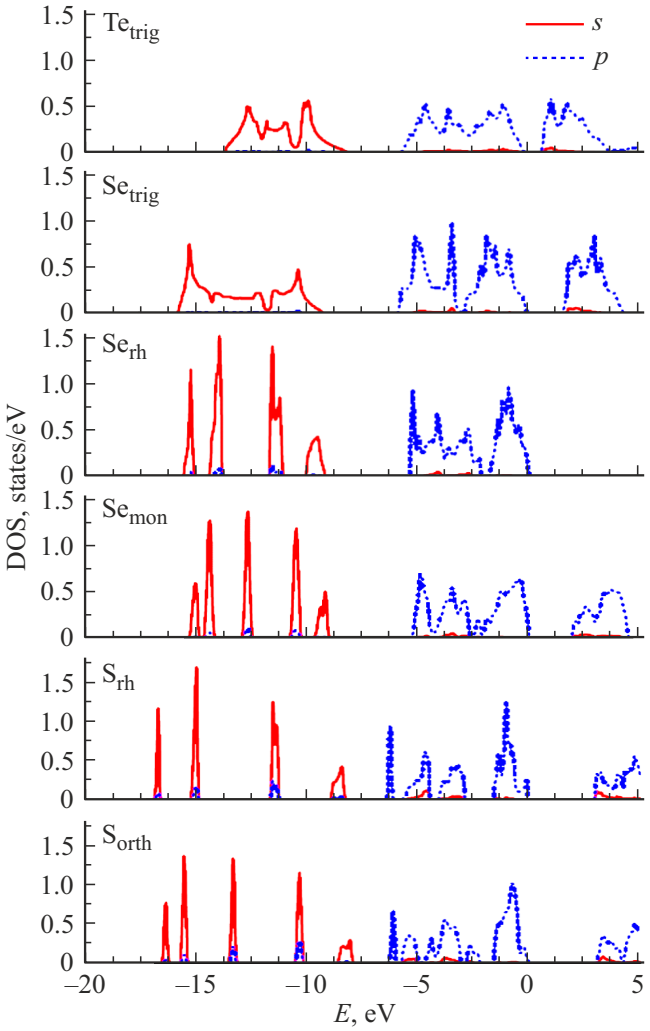

Figure 1. Partial DOS for valence s- and p-electrons in chalcogen crystals.

with respect to which it was believed that they were involved in a chemical bond. At the same time, there is a noticeable overlap in the zones of valence p-electrons in the trigonal Te. In rhombohedral S, the zones of valence p-electrons are divided into four subzones, and on the DOS of orthorhombic α-S, five subzones of valence p-electrons are visible. The positions and intensities of the DOS maxima for s- and p-electrons in Fig. 1 are in qualitative agreement with the features of experimental X-ray photoelectron spectra (XPS) and ultraviolet photoelectron spectra (UPS) for trigonal Te [43,44], trigonal, rhombohedral and monoclinic α-Se [40–43] and for orthorhombic α-S [40,42].

The values of the calculated energy gaps presented in Table 1 are in good agreement with the experimental data for chalcogen crystals. We could not find published experimental data for the energy gap in the rhombohedral S, so the calculated value of 2.9 eV may be a guideline for experiments.

Table 1. Calculated and experimental energy gaps in chalcogen crystals

Substance	Calculated energy gap, eV	The experimental energy gap at 300 K, eV	Source
Te, trigonal	0.2	0.323	[45]
Se, trigonal	1.45	1.6	[46]
Se, rhombohedral	1.75	1.9	[47]
α-Se, monoclinic	2.0	2.1	[48]
S, rhombohedral	2.9		
α-S, orthorhombic	3.0	2.9	[49]

Table 2. Characteristics of BCPs in crystals of trigonal Te and Se, as well as rhombohedral Se and S

Substance, spatial group	Type positions	N BCPs	d, Å	$\lvert\lambda_{1,2}\rvert/\lambda_3$	$\nabla^2\rho_b$ e/Å^5	ρ_b e/Å^3	η	s, %	p_1, %	p_u, %	f, %	μ
Te, trigonal $P3_121$ or $P3_221$	3*b*	2	2.835	0.58	−0.32	0.44	0.67	34	66		3.0	0.69
	6*c*	4	3.495	0.24	0.63	0.14	0.24	20	80			
Se, trigonal $P3_121$ or $P3_221$	3*b*	2	2.373	0.82	−1.72	0.69	0.74	41	46	13	1.5	0.87
	6*c*	4	3.436	0.19	0.74	0.09	0.10	16	44	40		
Se, rhombohedral $R\bar{3}$	6*f*	2	2.356	0.87	−2.00	0.72	0.74	41	49	10	0.9	0.95
	6*f*	2	3.414	0.18	0.76	0.10	0.10	17	50	33		
	3*e*	1	3.466	0.15	0.64	0.07	0.06	20	64	16		
	6*f*	2	3.964	0.14	0.35	0.04	0.03	10	39	51		
S, rhombohedral $R\bar{3}$	6*f*	2	2.057	2.20	−8.30	1.17	0.89	50	40	10	0.7	0.97
	6*f*	2	3.501	0.14	0.61	0.06	0.05	16	51	33		
	3*d*	1	3.749	0.10	0.53	0.05	0.04	12	38	50		
	3*e*	1	3.526	0.14	0.52	0.04	0.03	18	65	17		
	6*f*	2	3.850	0.13	0.37	0.03	0.03	11	35	54		

3.2. Characteristics of the bond critical points and charge density distribution in rhombohedral Se and S

The parameters of bond-type critical points (BCPs) in the charge density distribution in crystals of trigonal Se and Te, as well as in rhombohedral Se and S are presented in Table 2. In particular, Table 2 shows: the spatial group describing the symmetry of the crystal, the positions of high symmetry (Wyckoff positions) occupied by BCPs in the crystal structure, the number of each type of BCPs for nonequivalent atoms in the unit cell (N BCPs), interatomic distances d between bound atoms, calculated Bader characteristics [36–39] of BCPs (ratio of principal eigenvalues of the Hesse matrix $|\lambda_{1,2}|/\lambda_3$, laplacian value $\nabla^2\rho_b$, charge density ρ_b), values of the electron localization function (ELF) [50] in BCPs $\eta(\mathbf{r}_b)$, contributions of s-electrons, low-lying p_l- and overlying p_u-electrons in ρ_b, flatness f and molecularity μ. For trigonal Te, due to the overlap of the low-lying and overlying zones of valence p-electrons (see Fig. 1), Table 2 shows only the total contribution of p-electrons to ρ_b. The intervals of the low-lying p_l and overlying p_u zones of valence p-electrons were approximately determined (see Fig. 1) for the trigonal Se from −6 to −3 eV and from −3 eV to 0, and for rhombohedral Se and S from −6 to −2 eV and from −2 eV to 0, respectively.

In the unit cell of trigonal Te and Se, as well as rhombohedral Se and S, there is only one type of positions for nonequivalent atoms [9,10,25,26]. The total number of BCPs of all types per atom in the formula unit, N_{at}, for trigonal Te and Se coincides with the number of valence electrons in atoms and is equal to six, while for less

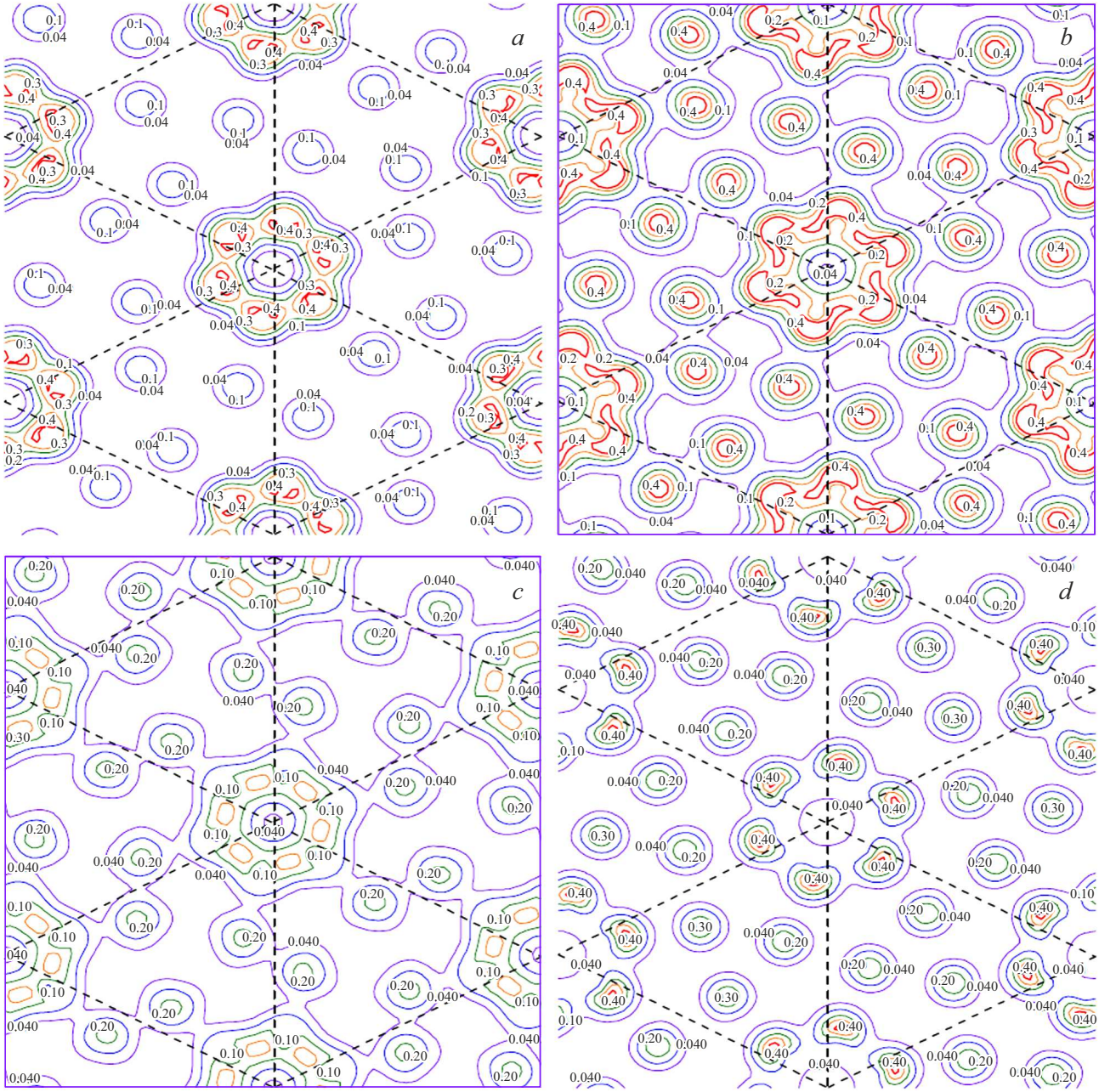

Figure 2. Contributions of valence s- and p-electrons to the charge density distribution (e/Å^3) in BCPs areas for rhombohedral Se: a — s-electrons, b —p-electrons, c — low-lying p_l-electrons, d — overlying p_u-electrons.

symmetric rhombohedral Se and S N_{at} is equal to seven and eight, respectively.

It follows from Table 2 that trigonal Te and Se have two types of BCPs with significantly different Bader parameters [18,19]. Valence s- and low-lying p_l-electrons contribute approximately equally to ρ_b of the first type BCPs in trigonal Se, while low-lying p_l- and upper p_u-electrons provide the main contribution to ρ_b of the second BCPs type [19]. In the rhombohedral Se, the values of the Bader parameters of the first two BCPs are close to the values of the parameters of the two BCPs in the trigonal Se. The contributions of valence s- and p-electrons in ρ_b of the first and second types of BCPs in rhombohedral Se are also similar to the corresponding contributions in trigonal Se. The partial contributions of valence s- and p-electrons to the charge density distribution in BCPs areas in rhombohedral Se are shown in Fig. 2.

The plane of Fig. 2 coincides with the base plane (a, b) of the unit cell of the rhombohedral Se in the hexagonal axes. 6 BCPs of the first type are located in this plane. They provide a bond between Se atoms in a six-branched ring. Three of these six Se atoms with coordinates $(0.042, 0.202, 0.120)$,

Table 3. Averaged BCPs characteristics for crystals of monoclinic α-Se and orthorhombic α-S

Substance, spatial group	Type positions	d, Å	$\lvert\lambda_{1,2}\rvert/\lambda_3$	$\nabla^2\rho_b$, e/Å^5	ρ_b, e/Å^3	η	f, %	μ	N_{at}
α-Se, monoclinic $P12_1/n1$	4*e*	2.34	0.91	−2.27	0.75	0.70	0.6	0.98	$N_{Se1} = 8$
	4*e*	3.63	0.16	0.56	0.06	0.06			$N_{Se2} = 7$
	2*d*	3.83	0.16	0.46	0.05	0.05			$N_{Se3} = 7$
	4*e*	3.87	0.13	0.42	0.04	0.04			$N_{Se4} = 8$
	2*c*	4.27	0.11	0.21	0.02	0.02			$N_{Se5} = 8$
	2*b*	4.27	0.07	0.17	0.01	0.01			$N_{Se6} = 6$
	4*e*	4.49	0.06	0.17	0.01	0.01			$N_{Se7} = 9$
									$N_{Se8} = 8$
α-S, orthorhombic $Fddd$	16*g*	2.04	3.62	−8.39	1.16	0.81	0.3	0.99	$N_{S1} = 7$
	32*h*	2.05	3.43	−8.25	1.16	0.81			$N_{S2} = 9$
	16*f*	3.38	0.16	0.69	0.06	0.05			$N_{S3} = 8$
	16*e*	3.41	0.16	0.65	0.06	0.04			$N_{S4} = 9$
	32*h*	3.71	0.14	0.42	0.04	0.02			
	16*f*	3.77	0.14	0.36	0.03	0.02			
	32*h*	3.86	0.14	0.33	0.03	0.02			
	16*c*	4.03	0.13	0.27	0.02	0.02			
	16*g*	4.12	0.12	0.22	0.02	0.01			
	16*d*	4.38	0.09	0.11	0.01	0.01			

$(-0.202, -0.160, 0.120)$, $(0.160, -0.042, 0.120)$ are above the base plane, and the other three atoms of the Se ring with coordinates $(-0.042, -0.202, -0.120)$, $(0.202, 0.160, -0.120)$, $(-0.160, 0.042, -0.120)$ located below the base plane [25]. In addition to the Se atoms forming the central ring, six other Se atoms are visible in the plane of Fig. 2, which belong to neighboring six-branched rings. Three of them are located above the base plane and have coordinates $(0.625, 0.131, 0.213)$, $(0.869, 0.494, 0.213)$, $(0.506, 0.375, 0.213)$. The other three atoms are located below the base plane and have coordinates $(0.375, 0.869, -0.213)$, $(0.131, 0.506, -0.213)$, $(0.494, 0.625, -0.213)$. BCPs of the second type, providing connections between six-branched rings in a rhombohedral Se, are located in planes spaced from the base plane by $\pm 0.059c$. They are located between the Se atoms of the central ring and the Se atoms of neighboring rings located in planes with the coordinate z equal to $\pm 0.213c$. BCPs of the third type are located in the base plane between Se atoms localized in planes spaced from the base plane by $\pm 0.213c$. The surroundings of BCPs of the first, second and third types are clearly visible in Fig. 2. BCPs of the fourth type for rhombohedral Se with a minimum value of $\rho_b = 0.035$ e/Å^3 do not fall into the plane of Fig. 2.

The BCPs characteristics in crystals of monoclinic α-Se and orthorhombic α-S averaged over groups of BCPs with the same symmetry of positions in the crystal and close interatomic distances are presented in Table 3. The contributions of valence s- and p-electrons to the charge density of ρ_b in BCPs are not presented in Table 3 due to similarity with the corresponding contributions for rhombohedral Se and S in Table 2.

It should be noted that in crystals of monoclinic α-Se there are eight types of positions for Se atoms [27], and in orthorhombic α-S — four types of positions for S atoms [28]. The last column of Table 3 shows the numbers N_{at} of BCPs for each position of nonequivalent atoms in the unit cell of the crystal. In total, in the crystals α-Se and α-S, the CRITIC2 program found 32 and 18 types of BCPs, respectively. Some of these types of BCPs, having the same symmetry and similar parameters, we have combined into groups according to the type of symmetry.

From the Table 2 and 3 it follows that in trigonal Te and Se there are two types of BCPs with significantly different Bader characteristics, while in molecular crystals of allotropic modifications of Se and S with a less symmetrical crystal structure there are significantly more types of BCPs. It is also significant that in less symmetric allotropic modifications of Se and S N_{at} exceeds the number of valence s- and p-electrons in atoms. A similar feature was previously found in bismuth and antimony chalcogenides with a low symmetry of the crystal structure [51].

3.3. Estimation of the influence of Van der Waals forces on BCPs characteristics in rhombohedral Se

To identify the influence of Van der Waals forces on the charge density distribution in rhombohedral Se, calculations of the electronic band structure were performed using the WIEN2k software package and the exchange-correlation functional rev-vdW-DF2 [33] recommended in [34]. For comparison, the exchange-correlation PBE functional [30] was also used in calculations. To complete the picture,

Table 4. Characteristics of BCPs in rhombohedral Se

Lattice parameters	E_{xc}	a, Å	c, Å	Position type	d, Å	$\lvert\lambda_{1,2}\rvert/\lambda_3$	$\nabla^2\rho_b$, e/Å^5	ρ_b, e/Å^3	f, %	μ
Experimental	PBE	11.362	4.429	$6f$	2.356	0.56	−0.50	0.68	1.4	0.94
				$6f$	3.414	0.18	0.68	0.10		
				$3e$	3.466	0.16	0.60	0.07		
				$6f$	3.964	0.14	0.33	0.04		
	rev-vdW-DF2	11.362	4.429	$6f$	2.356	0.56	−0.46	0.68	1.5	0.94
				$6f$	3.414	0.18	0.69	0.10		
				$3e$	3.466	0.16	0.61	0.07		
				$6f$	3.964	0.14	0.33	0.04		
Optimized	PBE	11.429	4.709	$6f$	2.398	0.54	−0.27	0.63	1.2	0.96
				$6f$	3.471	0.18	0.62	0.09		
				$3e$	3.546	0.16	0.53	0.06		
				$6f$	4.152	0.13	0.24	0.03		
	rev-vdW-DF2	11.472	4.497	$6f$	2.381	0.54	−0.31	0.65	1.4	0.94
				$6f$	3.450	0.18	0.65	0.09		
				$3e$	3.505	0.16	0.57	0.07		
				$6f$	4.019	0.14	0.30	0.04		

calculations of the electronic band structure were performed twice — with experimental values of the lattice parameters [25] and with optimized lattice parameters obtained using the procedure available in the WIEN2k computer software package. According to Hamada's article [33], Beke's improved exchange functional B86R (B86 — Beke's original exchange functional [52]) was chosen as the exchange energy E_x, and short-range LDA correlations — as the correlation energy. The Van der Waals forces were described in [33] using the nonlocal long-range correlation functional vdW-DF2 [53]. Charge density distributions in rhombohedral Se obtained after calculations of the electronic band structure were analyzed using the program CRITIC2 [35]. The characteristics of BCPs in rhombohedral Se are presented in Table 4. In particular, Table 4 shows: types of exchange-correlation functionals used in calculations, lattice parameters (experimental or optimized), high symmetry positions occupied by BCPs in the crystal lattice, interatomic distances d between bound atoms, calculated Bader characteristics of BCPs (ratio of the main values of the Hesse matrix $|\lambda_{1,2}|/\lambda_3$, laplacian value $\nabla^2\rho_b$, charge density in BCPs ρ_b), flatness f and molecularity μ.

Comparison of the Bader parameters of BCPs for rhombohedral Se, given in Table. 2 and 4, shows that the choice of the type of exchange-correlation functional for calculations of the electronic structure has a noticeable effect only on the value of the Laplacian of the charge density $\nabla^2\rho_b$ for BCPs of the first type, while the other two Bader parameters (the ratio of the main eigenvalues of the Hesse matrix $|\lambda_{1,2}|/\lambda_3$ and the charge density ρ_b), which determine the type of chemical bond in crystals, change slightly for BCPs of all types, including, taking into account the Van der Waals forces. Thus, it can be concluded that taking into account the Van der Waals forces does not change the types of chemical bonds in rhombohedral Se, as well as in trigonal Se [19]. This conclusion coincides with the remark made in [20]: „The nonlocal vdW potential has only a very small effect on the charge density and electronic structure and, consequently, is essential only for calculating the forces".

4. Discussion

To classify the types of chemical bonds in molecular chalcogen crystals, we will analyze the data presented in Tables 2, 3 and in Fig. 2, considering the peculiarities in the distribution of charge density in substances studied by us in the articles [18,19,51,54,55].

Rhombohedral Se and S have a greater number of BCPs types compared to trigonal Se and Te, are characterized by higher values of the BCPs numbers per atom, N_{at}, and the molecularity μ, as well as a smaller flatness of the charge density distribution f. Bader parameters of BCPs, values ELF $\eta(\mathbf{r}_b)$ and the pattern of charge density distribution in BCPs areas in rhombohedral Se, shown in Fig. 2, indicate the similarity of the characteristics of the first two types of BCPs in rhombohedral and trigonal Se. The third and fourth types of BCPs in rhombohedral Se, which provide a connection between six-branched rings of atoms, have significantly lower values of ρ_b than the first two types of BCPs, as well as almost zero values of $\eta(\mathbf{r}_b)$. Taking into account the fact that N_{at} in rhombohedral Se is greater than the number of valence electrons in the Se atom, it can be assumed that in rhombohedral Se there is another type of chemical bond characterized by the possibility of charge density fluctuations. As an example of such a chemical bonding mechanism, we can point to a recently proposed mechanism involving charge density fluctuations, the so-called „charge-shift bonding" [56,57]. Thus, three types

of chemical bonds coexist in rhombohedral Se: covalent (BCPs of the first type), semi-metallic (BCPs of the second type) and fluctuating (BCPs of the third and fourth types). A similar classification of BCPs types can be applied to the monoclinic α-Se, in which the structural units are eight-branched rings of Se atoms.

Calculations of the electronic band structure of the rhombohedral S were performed in [58] using the self-consistent method of the extended linearized augmented plane wave (ELAPW) and the exchange-correlation potential LDA. Consequently, the DOS picture for rhombohedral S in [58] is only in qualitative agreement with the data for rhombohedral S presented in Fig. 1. For example, the energy gap in [58] has about 30% lower value compared to the one obtained in this paper, which is a well-known disadvantage of LDA. A similar value of the energy gap in the orthorhombic α-S, reduced by 30% compared to the experimental and found by us, was obtained in the work [12] when calculating the electronic structure by the method of a full-potential linearized augmented plane wave (FLAPW) and using the exchange-correlation PBE functional.

Sulfur has a large number of allotropic modifications — polymer chains and molecular crystals consisting of rings with a number of links from 6 to 20 [59]. All molecular crystals have low symmetry: rhombohedral, orthorhombic, monoclinic, triclinic [59]. As follows from our analysis (see Table. 2 and 3), the charge density distribution in chalcogen crystals with low symmetry is characterized by the number of BCPs per atom exceeding the number of valence electrons in the atom, which can lead to charge density fluctuations. On the other hand, the degree of covalence of BCPs of the first type in rhombohedral and orthorhombic S is significantly higher than in trigonal, rhombohedral and monoclinic Se. Special attention is drawn to the very large values of $\nabla^2\rho_b$, ρ_b and $\eta(\mathbf{r}_b)$ in BCPs, which connect atoms in six- and eight-branched rings of sulfur molecular crystals. At the same time, the parameters of other types of BCPs in rhombohedral and orthorhombic sulfur, which provide connections between neighboring rings, have lower values compared to the corresponding parameters of allotropic modifications of Se. The above assumption about the coexistence of three types of chemical bonds in rhombohedral and monoclinic Se can also be applied to rhombohedral and orthorhombic sulfur.

Our analysis of the charge density distribution features in Se and S molecular crystals did not reveal the presence of any other BCPs inside the rings of atoms, except for BCPs of the first type, which is consistent with the results of quantum chemical calculations for large rings of Se and S [60] atoms, as well as with experimental studies of the charge density distribution in the orthorhombic α-S, performed by X-ray and neutron scattering methods [59].

We note that recent studies of high-temperature superconductors (HTS) by the method of resonant inelastic X-ray scattering (RIXS) [61] have revealed the presence of dynamic short-range charge density fluctuations with a characteristic energy of the order of several meV in almost all families of HTS. A possible reason for the occurrence of such fluctuations in charge density can be found earlier in bismuth and antimony chalcogenides [51], as well as in unusual (including HTS) superconductors [55] a feature of the nature of the chemical bond — the total number of BCPs per atom exceeds the number of valence electrons in the atom. Since we have also found this feature in the chemical bond in chalcogen molecular crystals, it would be desirable to study them by the RIXS method in order to experimentally search for the presence of charge density fluctuations in them.

5. Conclusions

The analysis of the charge density distribution in rhombohedral Se and S, monoclinic α-Se and orthorhombic α-S showed that valences- and low-energy p_l-electrons contribute almost equally to the charge density of BCPs binding the nearest neighboring atoms, while low-lying p_l- and overlying p_u-electrons provide a bond between the rings of Se and S atoms in molecular crystals. In addition to the covalent and semi-metallic types of chemical bonds realized in trigonal Se and Te, there also appears to be a third type of chemical bond in chalcogen molecular crystals, which is characterized by the possibility of charge density fluctuations. Van der Waals forces in molecular chalcogen crystals contribute to the equilibrium values of the crystal lattice parameters, but have little effect on the BCPs parameters that determine the type of chemical bond.

Funding

The work was carried out using the equipment of the center for collective use „Complex of modeling and data processing of mega-class research facilities“ NRC „Kurchatov Institute“, http://ckp.nrcki.ru/.

Conflict of interest

The authors declare that they have no conflict of interest.

References

[1] Application of Chalcogenides: S, Se, and Te / Ed. G.K. Ahluwalia. Springer International Publishing, Cham (2017).
[2] M. Hirayama, R. Okugawa, S. Ishibashi, S. Murakami, T. Miyake. Phys. Rev. Lett. **114**, 206401 (2015).
[3] M. Sakano, M. Hirayama, T. Takahashi, S. Akebi, M. Nakayama, K. Kuroda, K. Taguchi, T. Yoshikawa, K. Miyamoto, T. Okuda, K. Ono, H. Kumigashira, T. Ideue, Y. Iwasa, N. Mitsuishi, K. Ishizaka, S. Shin, T. Miyake, S. Murakami, T. Sasagawa, T. Kondo. Phys. Rev. Lett. **124**, 136404 (2020).
[4] S.S. Tsirkin, I. Souza, D. Vanderbilt. Phys. Rev. B **96**, 045102 (2017).
[5] Y.-H. Chan, B. Kilic, M.M. Hirschmann, C.-K. Chiu, L.M. Schoop, D.G. Joshi, A.P. Schnyder. Phys. Rev. Mater. **3**, 124204 (2019).

[6] K. Nakayama, M. Kuno, K. Yamauchi, S. Souma, K. Sugawara, T. Oguchi, T. Sato, T. Takahashi. Phys Rev. B **95**, 125204 (2017).
[7] G. Gatti, D. Gosálbez-Martínez, S.S. Tsirkin, M. Fanciulli, M. Puppin, S. Polishchuk, S. Moser, L. Testa, E. Martino, S. Roth, Ph. Bugnon, L. Moreschini, A. Bostwick, C. Jozwiak, E. Rotenberg, G. Di Santo, L. Petaccia, I. Vobornik, J. Fujii, J. Wong, D. Jariwala, H.-A. Atwater, H.M. Rønnow, M. Chergui, O.V. Yazyev, M. Grioni, A. Crepaldi. Phys. Rev. Lett. **125**, 216402 (2020).
[8] International Tables for Crystallography. Volume A. Space group symmetry / Ed. Th. Hahn. Springer, Dordrecht (2005).
[9] P. Cherin, P. Unger. Acta Crystallogr. **23**, 670 (1967).
[10] P. Cherin, P. Unger. Inorg. Chem. **6**, 1589 (1967).
[11] L. Yang, Z.-G. Chen, M.S. Dargusch, J. Zou. Adv. Energy Mater. **8**, 1701797 (2018).
[12] H. Momida, T. Yamashita, T. Oguchi. J. Phys. Soc. Jpn **83**, 124713 (2014).
[13] E. Mooser, W.P. Pearson. Can. J. Phys. **34**, 1369 (1956).
[14] M. Kastner. Phys. Rev. Lett. **28**, 355 (1972).
[15] G. Lucovsky, R.M. White. Phys. Rev. B **8**, 660 (1973).
[16] L. Pauling. The nature of the Chemical bond. Cornell Univ. Press, Itaca, N.Y. (1960).
[17] J.D. Joannopoulos, M. Shlüter, M.L. Cohen. Phys. Rev. B **11**, 2186 (1975).
[18] V.G. Orlov, G.S. Sergeev. Fizika Tverdogo Tela **59**, 1278 (2017).
[19] V.G. Orlov, G.S. Sergeev. AIP Adv. **12**, 055110 (2022).
[20] P. Blaha, K. Schwarz, G.K.H. Madsen, D. Kvasnicka, J. Luitz, R. Laskowski, F. Tran, L.D. Marks. WIEN2k, An Augmented Plane Wave + Local Orbitals Program for Calculating Crystal Properties. Vienna University of Technology, Vienna (2018). ISBN 3-9501031-1-2.
[21] P. Blaha, K. Schwarz, F. Tran, R. Laskowski, G.K.H. Madsen, L.D. Marks. J. Chem. Phys. **152**, 074101 (2020).
[22] F. Tran, P. Blaha. Phys. Rev. Lett. **102**, 226401 (2009).
[23] W. Han, P. Huang, L. Li, F. Wang, P. Luo, K. Liu, X. Zhou, H. Li, X. Zhang, Y. Cui, T. Zhai. Nature Commun. **10**, 4728 (2019).
[24] Ch. Tan, X. Cao, X.-J. Wu, Q. He, J. Yang, X. Zhang, J. Chen, W. Zhao, Sh. Han, G.-H. Nam, M. Sindoro, H. Zhang. Chem. Rev. **117**, 6225 (2017).
[25] Y. Miyamoto. Jap. J. Appl. Phys. **19**, 1813 (1980).
[26] J. Donohue, A. Caron, E. Goldish. J. Am. Chem. Soc. **83**, 3748 (1961).
[27] P. Cherin, P. Unger. Acta Crystallogr. B **28**, 313 (1972).
[28] A.S. Cooper. Acta Crystallogr. **15**, 578 (1962).
[29] H. Dixit, R. Saniz, S. Cottenier, D. Lamoen, B. Partoens. J. Phys. Condens. Matter **24**, 205503 (2012).
[30] J.P. Perdew, K. Burke, M. Ernzerhof. Phys. Rev. Lett. **77**, 3865 (1996).
[31] J.P. Perdew, K. Schmidt. AIP Conf. Proc. **577**, 1 (2001).
[32] J.P. Perdew, A. Ruzsinszky, J. Tao, V.N. Staroverov, G. Scuseria, G.I. Csonka. J. Chem. Phys. **123**, 062201 (2005).
[33] I. Hamada. Phys. Rev. B **89**, 121103(R) (2014).
[34] F. Tran, L. Kalantari, B. Traore, X. Rocquefelte, P. Blaha. Phys. Rev. Mater. **3**, 063602 (2019).
[35] A. Otero-de-la-Roza, E.R. Johnson, V. Luaña. Comput. Phys. Commun. **185**, 1007 (2014).
[36] R.F.W. Bader. Atoms in Molecules: A Quantum Theory. International Series of Monographs on Chemistry 22. Oxford Science Publications, Oxford (1990).
[37] C. Gatti. Z. Kristallogr. Cryst. Mater. **220**, 399 (2005).
[38] The Quantum Theory of Atoms in Molecules. From Solid State to DNA and Drug Design / Ed. C.F. Matta, R.J. Boyd. Wiley-VCN, Weinheim (2007).
[39] P. Mori-Sánchez, A.M. Pendás, V. Luaña. J. Am. Chem. Soc. **124**, 14721 (2002).
[40] W.R. Salaneck, C.B. Duke, A. Paton, C. Griffiths, R.C. Keezer. Phys. Rev. B **15**, 1100 (1977).
[41] T. Takahashi, K. Murano, K. Nagata, Y. Miyamoto. Phys. Rev. B **28**, 4893 (1983).
[42] W.R. Salaneck, N.O. Lipari, A. Paton, R. Zallen, K.S. Liang. Phys. Rev. B **12**, 1493 (1975).
[43] M. Schlüter, J.D. Joannopoulos, M.L. Cohen, L. Ley, S.P. Kowalczyk, R.A. Pollak, D.A. Shirley. Solid State Commun. **15**, 1007 (1974).
[44] M. Taniguchi, M. Tamura, Y. Hari, H. Sato, M. Nakatake, H. Namatame, S.Hosokawa, Y. Ueda. J. Phys. Condens. Matter. **6**, 5181 (1994).
[45] V.B. Anzin, M.I. Eremets, Yu.V. Kosichkin, A.I. Nadezdinskii, A.M. Shirokov. Phys. Status Solidi A **42**, 385 (1977).
[46] M. Taniguchi. J. Alloys Compd. **286**, 114 (1999).
[47] K. Nagata, Y. Miyamoto, H. Nishimura, H. Suzuki, S. Yamasaki. Jpn. J. Appl. Phys. **24**, L858 (1985).
[48] H. Luo, S. Degreniers, Y.K. Vohra, A.L. Ruoff. Phys. Rev. Lett. **67**, 2998 (1991).
[49] R.F.W. Bader, W.H. Henneker, P. Cade. J. Chem. Phys. **46**, 3341 (1967).
[50] A.D. Becke, K.A. Edgecombe. J. Chem. Phys. **92**, 5397 (1990).
[51] V.G. Orlov, G.S. Sergeev, E.A. Kravchenko. J. Magn. Magn. Mater. **475**, 627 (2019).
[52] A.D. Becke. J. Chem. Phys. **85**, 7184 (1986).
[53] K. Lee, É.D. Murray, L. Kong, B.I. Lundqvist, D.C. Langreth. Phys. Rev. B **82**, 081101(R) (2010).
[54] V.G. Orlov, G.S. Sergeev. Solid State Commun. **258**, 7 (2017).
[55] V.G. Orlov, G.S. Sergeev. Physica B **536**, 839 (2018).
[56] S. Shaik, D. Danovich, W. Wu, P.C. Hiberty. Nature Chem. **1**, 443 (2009).
[57] S. Shaik, D. Danovich, J.M. Galbraith, B. Braïda, W. Wu, P.C. Hiberty. Angew. Chem. Int. Ed. **59**, 984 (2020).
[58] O.V. Krasovska, B. Winkler, E.E. Krasovskii, V.N. Antonov, B.Yu. Yavorsky. J. Phys. Condens. Matter **10**, 4093 (1998).
[59] R. Stendel, B. Eckert. In: Elemental sulfur and sulfur-rich compounds I. Topics in Current Chemistry V. 230 / Ed. R. Stendel. Springer, Berlin, Heidelberg (2003). https://doi.org/10.1007/b12110
[60] R. Gleiter, G. Haberhauer, F. Rominger. Eur. J. Inorg. Chem. **34**, 3846 (2019).
[61] R. Arpaia, S. Caprara, R. Fumagalli, G. De Vecchi, Y.Y. Peng, E. Andersson, D. Betto, G.M. De Luca, N.B. Brookes, F. Lombardi, M. Salluzzo, L. Braicovich, C. Di Castro, M. Grilli, G. Ghiringhelli. Science **365**, 906 (2019).